Chemical Science

Accepted Manuscript

This article can be cited before page numbers have been issued, to do this please use: S. Roy, S. Tyagi and P. P. Pillai, *Chem. Sci.*, 2026, DOI: 10.1039/D6SC01862A.

ROYAL SOCIETY OF CHEMISTRY

rsc.li/chemical-science

View Article Online
DOI: 10.1039/D6SC01862A

EDGE ARTICLE

Kinetically Programmed Pathway-Dependent Autonomous Reversibility in Biomimetic Self-Assembly of Nanoparticles

Received 00th January 20xx,
Accepted 00th January 20xx

DOI: 10.1039/x0xx00000x

Sumit Roy,[a] Shreya Tyagi,[a] and Pramod P. Pillai*[a]

Abstract: Autonomous reversibility is fundamental to many natural systems, enabling the formation of dynamic and adaptive assemblies without continuous external intervention. Replicating autonomous behavior in artificial systems remains challenging, as it demands a kinetic imbalance in the self-assembly process driven by chemically triggered dynamic interactions. Here, we demonstrate pathway-dependent autonomous reversibility in a bio–nano hybrid system composed of adenosine triphosphate (ATP) and gold nanoparticles (AuNPs), with hexokinase (HK) as an enzymatic disassembling trigger. The electrostatic interaction between oppositely charged AuNPs and ATP drives co-assembly, while HK-mediated dephosphorylation of ATP to ADP weakens these interactions, inducing rapid disassembly. Autonomous reversibility is achieved via two distinct pathways. In pathway I, excess HK promotes autonomous disassembly, with ATP addition triggering the transient assembly. Conversely, in pathway II, an excess of ATP maintains autonomous assembly, with transient disassembly driven by HK-mediated dephosphorylation. Thus, using the same constituent components under distinct conditions, we demonstrate both transient assembly and transient disassembly within a single system. Interestingly, the autonomous assembly and disassembly pathways determine the nature of the self-assembled state – either a precipitate or a plasmonically active, controlled aggregate is formed. The lifetime of these transient states is tuned from minutes to hours by balancing the competing kinetics of ATP and HK triggers, offering a versatile platform for temporal control in applications such as transient catalysis and other time-programmed functions.

Introduction

Many natural processes employ autonomous reversibility as a key mechanism to achieve their functions, including the schooling of fish, the operation of molecular machinery, and the repair of self-healing tissues.[1-6] The realization of autonomous behavior in artificial self-assembled systems remains a key challenge in supramolecular chemistry, as it requires a temporal modulation of assembly and disassembly kinetics to enable dynamic and reversible transitions with minimal external intervention.[7-10] Achieving this level of control requires an intricate balance between opposing processes, where one trigger dominates the system while the opposing trigger is only transiently active.[11-14] In principle, such a kinetic imbalance in the self-assembly process can be achieved using an excess of disassembling trigger (pathway I) or an excess of assembling trigger (pathway II), while allowing transient dominance of the counter trigger. In biological systems, these pathways are achieved through precisely controlled, enzymatic cascade reaction networks that dynamically regulate the interactions among molecular building blocks.[15,16] For instance, the GTP- and ATP-fueled dynamic self-assembly of microtubules and actin filaments are classic examples of pathway I, while fibrin self-assembly during blood clotting and collagen organization in the extracellular matrix exemplify pathway II.[17-20]

Translating such pathways into synthetic systems demands the design of programmable platforms in which assembly and disassembly cycles can proceed autonomously through chemically encoded instructions.[21-30] Even though limited, success has been achieved in realizing autonomous self-assembly, with complete redispersal, using pathway I with both molecular and nanomaterial building blocks.[31-44] George and co-workers designed a bio-inspired artificial supramolecular system that exhibits transient and switchable helicity in an autonomous fashion, using an *"enzyme-in-tandem"* approach.[45] In another study, Klajn and co-workers have regulated the ATP-triggered co-assembly with AuNPs in the presence of excess dephosphorylating enzyme to achieve an autonomous shuttling between dispersed and non-functional amorphous aggregates.[46] On the other hand, in pathway II, disassembly is inherently difficult due to the kinetic bias toward assembly when the aggregating trigger is in excess, thereby halting the process at the assembled state. This likely could be the reason for the lack of reports on autonomous artificial self-assembly systems via pathway II. The challenge is further amplified when nanomaterials serve as building blocks, as in the case of gold nanoparticles. Owing to the high Hamaker constant of gold, the van der Waals interactions within the assembled state are especially strong, making disassembly under the dominance of assembling trigger conditions via pathway II even more

[a] Department of Chemistry, Indian Institute of Science Education and Research (IISER), Dr. Homi Bhabha Road, Pune – 411 008, India.
Email: pramod.pillai@iiserpune.ac.in

† Supplementary Information available: See DOI: 10.1039/x0xx00000x

unfavorable.[47] As is clear from the literature, mimicking temporal control over the kinetics of assembly and disassembly steps in artificial systems remains a formidable challenge.[48]

Here, we report a pathway-dependent autonomous reversibility in an artificial bio–nano hybrid system by controlling the kinetics between assembly and disassembly steps using both pathways I and II. Oppositely charged AuNPs and ATP were chosen as building block and aggregating trigger, respectively, because of their rich properties that support the formation of functional assembled states, as well as their pH-dependent aggregation behavior (*vide infra*).[45,49] Further, their complementary surface charges enable precise modulation of assembly and disassembly kinetics through electrostatic interactions. Addition of anionic ATP to a solution of [+] AuNPs induced instant co-assembly, leading to a complete precipitation of the AuNPs within ~8 h. Disassembly was triggered by hexokinase (HK), which enzymatically dephosphorylates ATP to ADP within the co-assembled aggregates, thereby weakening the electrostatic interactions and rapidly redispersing the AuNPs (**Scheme 1**). We implemented pathway I (transient assembly)-driven autonomous self-assembly using HK-disassembling trigger in excess to favor disassembly, while allowing transient dominance of ATP-triggered assembly. This created a non-equilibrium condition, enabling multiple autonomous reversible cycles. In contrast to the conventionally observed nanoparticle precipitates in the self-assembled state, discrete, colloidally stable, and plasmonically active aggregates were formed in Pathway I (transient assembly) via a controlled aggregation process. These aggregates are termed “controlled aggregates”. Further, we realized autonomous reversibility via pathway II (transient disassembly) by using ATP-aggregating trigger in excess to promote re-assembly, while allowing transient dominance of HK-mediated disassembly. This created a non-equilibrium condition wherein reversible cycling between aggregated and dispersed states occurred autonomously over multiple cycles (typically 3–8 cycles, depending on the ATP concentration). The transient activity of the opposing trigger in each pathway was achieved by operating the dominant trigger under unfavorable conditions. In short, we present a nanoparticle system that uniquely integrates both transient aggregation and transient dispersion in a single system, conceptually inspired by natural systems to achieve diverse functions from a limited set of biomolecular building blocks. Interestingly, the pathway used for achieving autonomous reversibility determined the nature of the self-assembled state: pathway I (transient assembly) enabled transitions between completely dispersed and plasmonically active, controlled aggregate states (*functional*), whereas pathway II (transient disassembly) facilitated reversible switching between completely dispersed and completely precipitated states (*non-functional*). Furthermore, precise control over the competing kinetics of ATP-induced aggregation and HK-triggered disassembly enabled tuning the lifetime of the controlled aggregate states from 20 min to 3 h. This offers a new strategy for engineering temporal functions in self-assembled systems. Given the rich properties of both ATP as well as plasmonic AuNPs and the system’s responsiveness to biochemical triggers, such co-assembled bio-nano hybrid platforms hold significant promise for achieving temporal functions under non-equilibrium conditions.

Results and Discussion

View Article Online
DOI: 10.1039/D6SC01862A

Design of biomimetic dynamic self-assembled system

To achieve autonomous reversibility, a temporal control over the dominance of assembly over the disassembly, and vice versa, is essential. This kinetic imbalance can be achieved by installing dynamic, tunable, and reversible interactions between judiciously selected building blocks and stimuli-responsive triggers. Gold nanoparticles (AuNPs) were chosen as the building blocks due to their rich surface chemistry and distinctive optoelectronic properties, which enable functional modulation across both assembled and disassembled states.

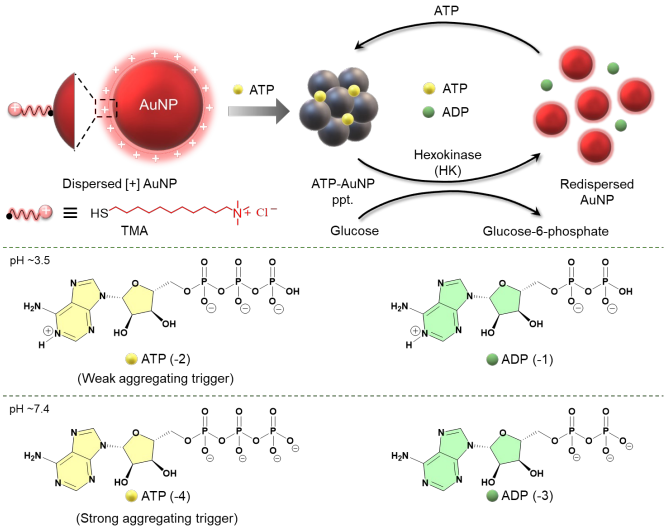

Scheme 1. Biomimetic dynamic self-assembly of AuNPs. The electrostatic attraction between oppositely charged ATP and AuNPs induces the co-assembly process, leading to the complete precipitation of AuNPs. The addition of the HK enzyme initiates the dephosphorylation of ATP to ADP, which weakens the electrostatic attraction, resulting in the disassembly of the precipitates and complete re-dispersal of AuNPs. This process enables reversible shuttling between completely dispersed and completely precipitated states of AuNPs. ATP and HK serve as the assembly and disassembly triggers, respectively, enabling autonomous dynamic control over the self-assembly process.

Adenosine triphosphate (ATP) was selected as the assembly trigger to induce assembly in nanoparticles due to its unique biochemical properties and pH-sensitive aggregation behavior, allowing precise tuning of assembly and disassembly kinetics. Previous studies have established that co-assembly between negatively charged ATP and positively charged AuNPs is predominantly driven by electrostatic interactions, which are highly sensitive to pH conditions.[45,49] The assembly kinetics is significantly influenced by the net charge on ATP, which in turn can be modulated by the pH. At physiological pH (7.4), ATP carries a net charge of –4, promoting rapid assembly through strong electrostatic attraction. In contrast, under acidic conditions (pH 3.5), protonation at the γ-phosphate and N1 positions reduces the net charge of ATP to –2, which significantly slows the assembly kinetics. Thus, the aggregation power of ATP to induce assembly in nanoparticles is intrinsically pH-

View Article Online
DOI: 10.1039/D6SC01862A

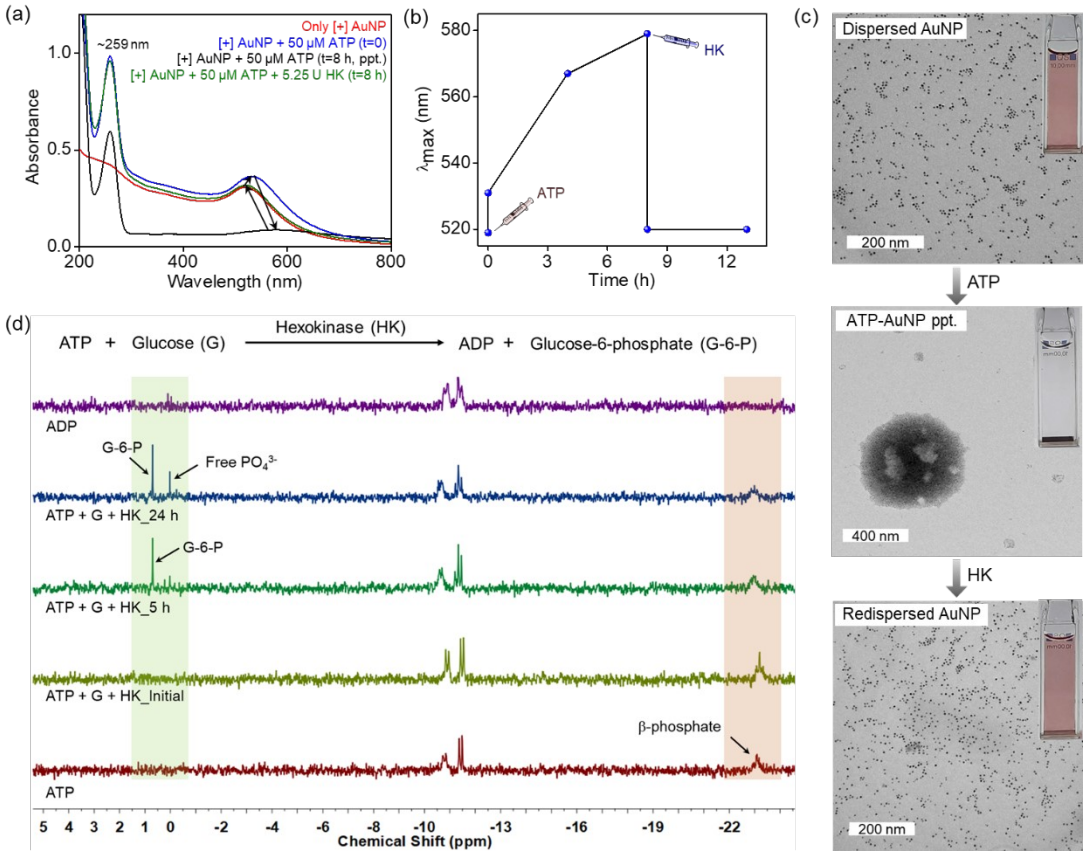

Figure 1. ATP-triggered dynamic self-assembly of AuNPs. (a) The absorption data depicts an instant aggregation of [+] AuNPs, followed by precipitation upon the addition of ~50 µM ATP (red to blue to black). The addition of 5.25 units of HK enzyme breaks the AuNP-ATP precipitate instantly to completely redisperse the NPs (green trace). The corresponding (b) variation in the λ_{max} with time for one assembly-disassembly cycle. (c) TEM images and optical photographs of the three different stages (dispersed, precipitate, and redispersed) involved in the ATP and HK enzyme-triggered self-assembly process of AuNPs. Impressively, a complete shuttling between plasmonically 'off' and 'on' states of AuNPs was achieved. (d) Time-dependent ^{31}P NMR was performed to monitor the phosphoryl transferase activity of the HK enzyme during the dynamic self-assembly process. The conversion of ATP and glucose (G) into ADP and glucose-6-phosphate (G-6-P), respectively, were monitored with time.

dependent, exhibiting strong activity at pH 7.4 and significantly reduced activity at pH 3.5. Additionally, phosphorylation-dephosphorylation can be another approach to regulate the aggregation ability of nucleotides, as the electrostatic interaction primarily emanates from the phosphate groups – the aggregation power follows the order ATP > ADP > AMP. Consequently, the aggregation power of ATP to induce assembly in nanoparticles can be fine-tuned by enzymatic dephosphorylation, adding another layer of control. This dual-level modulation, via pH and dephosphorylation, enables ATP to function as a programmable assembly trigger, capable of introducing temporal control in nanoparticle assembly and disassembly processes. These factors make ATP an ideal aggregation trigger to achieve autonomous reversibility in artificial self-assembly systems.

Our first objective was to test the suitability of pH modulation and enzymatic dephosphorylation as strategies to regulate the self-assembly of ATP with AuNPs. To this end, we synthesized cationic AuNPs functionalized with N,N,N-trimethyl(11-mercaptoundecyl)ammonium chloride ([+] AuNPs), which provides a stable positive surface charge through quaternary ammonium groups, enabling electrostatic interaction with anionic ATP (**Fig. S1**†, and **S2**†). This electrostatic driving force was chosen as the dynamic, tunable, and reversible interaction to mediate the assembly–disassembly processes under external pH or enzymatic stimuli. First, the pH dependent aggregation power of ATP was tested. For this, ~5 µM ATP (aggregating trigger) was added to a 3 mL aqueous dispersion of [+] AuNPs (~6 nM in terms of NPs; ~8 µM of TMA) at pH 3.5, where ATP has an overall -2 charge. No signs of aggregation of AuNPs were observed even after ~12 h (**Section 2**, and **Fig. S3a**†). Then, the pH was raised to ~7.4 where ATP attains -4 charge. As hypothesized, an immediate aggregation with a ~12 nm red shift in the plasmon maxima was observed, followed by a complete precipitation of AuNPs (**Fig. S3b**†). Interestingly, upon adjusting the pH back to 3.5, an immediate and complete redispersion of the AuNP-ATP precipitate was observed, with a ~22 nm blue shift in the plasmon maxima. These studies confirm that pH can be used as a tool to control the kinetics of ATP-triggered self-assembly processes.

Next, the suitability of the dephosphorylation pathway to achieve the dynamic self-assembly was tested. The minimum concentration of ATP required to drive the assembly of AuNPs (6 nM) in 3 mL at pH 3.5 was ~10 μM (**Fig. S4**†). To an aqueous dispersion of [+] AuNPs (~6 nM in terms of NPs) at pH 3.5, ~50 μM ATP (aggregating trigger) was added. This addition induced immediate aggregation of AuNPs, followed by the complete precipitation of the NPs (plasmonically off state) within ~8h (**Fig. 1a-c** and **S5**†). UV–vis absorption studies show an instant red shift (~10 nm) in the plasmon band after the addition of ~50 μM ATP, followed by the complete disappearance of plasmonic features, confirming the transition from dispersed to aggregated and precipitated states (**Fig. 1a**, **b** and **S5**†). A concomitant decrease in absorbance at ~259 nm (ΔAbs ~0.37), corresponding to the adenine chromophore of ATP, confirmed the incorporation of ATP into the AuNP precipitates. As hypothesized earlier, the enzymatic dephosphorylation of ATP to ADP would reduce the electrostatic attraction within co-assembled AuNPs, leading to disassembly and dynamicity in the system (**Scheme 1**). Accordingly, the AuNP-ATP precipitate was incubated at 37 °C with Hexokinase (HK, 5.25 units) and glucose (G ~250 equivalents. Glucose alone had a negligible effect on the nanoparticle self-assembly process. **Fig. S6**† and **S7**†). This resulted in an immediate redispersion of AuNPs, as evidenced by a blue shift of ~58 nm in the plasmon band (**Fig. 1b**). Interestingly, a complete transition from a '*plasmonically-off*' precipitate state to a '*plasmonically-on*' dispersed AuNP state was observed, with a complete revival of the plasmon band (**Fig. 1a**). Dynamic light scattering (DLS) and microscopy (SEM and TEM) studies corroborate well with the UV-vis absorption data, confirming the dynamicity and complete reversibility in the self-assembly process (**Fig. 1c**, **S8**†, and **S9**†). All these studies suggest that ATP dephosphorylation to ADP disrupts the ATP–AuNP electrostatic network, thereby leading to the complete disassembly. To directly monitor the dephosphorylation of ATP to ADP with HK enzyme, time-dependent ^{31}P NMR studies were performed under reaction conditions optimized for signal detection (2 mM ATP, 0.5 M G, and 70 units of HK/mL) (**Fig. 1d**). A significant decrease in peak corresponding to the β-phosphate of the ATP (at ~ -23 ppm) was observed with time, along with the formation of two new peaks corresponding to glucose-6-phosphate (at ~1 ppm) and free phosphate (~0.05 ppm). These results unambiguously confirm the enzymatic dephosphorylation of ATP into ADP, and the simultaneous phosphorylation of G to G-6-P. Thus, it can be concluded that ATP and HK act as assembling and disassembling triggers in our system, respectively. Their orthogonal and tunable actions provide a platform for temporal control over the dominance of assembly and disassembly steps, offering a viable route toward autonomous behavior in the self-assembly process. These efforts are summarized in subsequent sections.

Autonomous reversibility

Autonomous reversibility in self-assembly can be realized by installing autonomy in either the assembly or disassembly cycle using an excess of the respective trigger – referred to as pathway I (excess disassembling trigger) and pathway II (excess assembling trigger). More importantly, the long-term dominance of the excess trigger must be transiently counteracted by the opposing trigger to enable multiple, reversible assembly-disassembly cycles. For example, pathway I (transient assembly) requires that the dominant disassembling trigger be transiently suppressed by the assembling trigger to achieve similar autonomous reversibility. Conversely, in pathway II (transient disassembly), reaction conditions must be optimized such that the action of the excess assembling trigger is temporarily overcome by the disassembly trigger, thus permitting autonomous cycling between assembled and disassembled states (**Scheme 2**). Hence, the realization of autonomous reversibility requires a perfect balance between long-term dominance and transient suppression of the respective triggers, enabling dynamic control over the self-assembly process without constant external intervention.

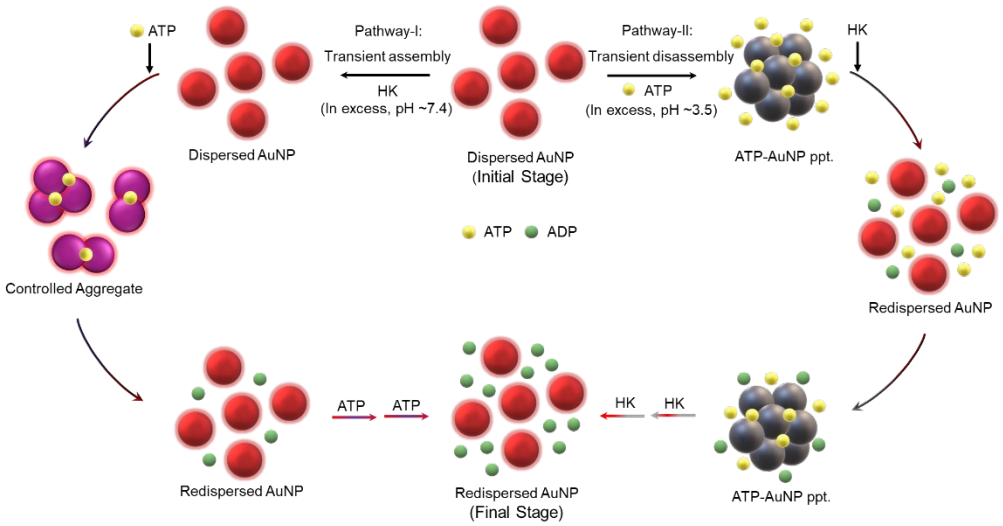

View Article Online
DOI: 10.1039/D6SC01862A

Scheme 2. Attaining autonomous reversibility in dynamic self-assembly process through two different assembly pathways: Pathway I is in the presence of excess disassembly trigger (HK enzyme), and pathway II is in the presence of excess assembly trigger (ATP).

Pathway I (transient assembly): Excess HK-driven autonomous reversibility

Pathway I (transient assembly) involves triggered assembly by ATP and autonomous disassembly by an excess of the disassembling trigger HK (**Scheme 2**). An excess of HK was added in the initial stage to achieve its long-term dominance over the opposing action of the assembling ATP trigger. To ensure the transient assembly in the presence of excess disassembling HK trigger, the self-assembly process was performed at pH ~7.4, where ATP exhibits strong aggregation capability (**Fig. 2a**). Under these conditions, disassembly proceeds autonomously without requiring continuous addition of the HK trigger, while assembly is initiated upon ATP addition. This interplay between the dominant disassembly pathway and transiently activated assembly enables multiple reversible cycles of aggregation and redispersion. In a typical experiment, assembly was initiated by adding ~5 μM ATP to a 3 mL mixture containing ~6 nM [+] AuNPs, ~0.36 units of HK, and ~250 equivalents of G at 37 ^{0}C. This induced instant aggregation, evidenced by a ~10 nm red shift in the plasmon band and a visual color change (**Fig. 2b, c, and S10**†). Unlike in pathway II (vide infra), the ATP-AuNP aggregation did not undergo complete precipitation due to the presence of excess disassembling HK trigger in solution. This led to the formation of a plasmonically active, controlled aggregate state (**Fig. 2a-c, and S11**†). Subsequently, the excess HK enzyme present in the system will disassemble ATP-AuNP controlled aggregates, leading to a complete redispersal (**Fig. 2b**). Notably, the purple color of the ATP-AuNP aggregate solution (λ_{max} ~537 nm) persisted for 20 min after ATP addition (representing a stagnant phase), before reverting to the original wine-red color (λ_{max} ~520 nm) within 40 min. Thus, the dominance of the disassembling cycle was regained soon after the transient dominance of the assembling ATP trigger. The next cycle was initiated by adding a fresh aliquot of 5 μM ATP, which led to the immediate aggregation followed by a stagnant phase corresponding to the controlled aggregate state (~40 min long-lived state). Now, the excess HK present in the solution will dominate the assembling action of ATP, ensuring the consistent disassembly of ATP-AuNP controlled aggregates. In this way, we were successful in achieving five reversible cycles with the triggered-assembly and autonomous-disassembly in the presence of ~0.36 units of HK (**Fig. 2d** and **S10**†). Specifically, the shuttling occurred between dispersed and plasmonically active, controlled aggregate states of AuNPs in an autonomous fashion. It must be noted that the kinetics of the autonomous disassembly slowed after each cycle. This can be attributed to the electrostatic attraction building between [+] AuNPs and the increasing concentration of anionic ADP generated after each cycle. Interestingly, the kinetics of the disassembling process depends on the activity/amount of HK trigger, allowing modulation of the lifetime of the plasmonically active, controlled aggregate state. In the presence of 0.06 units of HK enzyme, the controlled aggregate state *'lived'* for ~130 min before disassembly dominated, completing redispersion in ~270 min. Thus, only one cycle of triggered assembly and autonomous disassembly was observed in ~270 min with 0.06 units of HK. In comparison, 0.18 and 0.36 units of HK enzyme yielded two and three cycles of triggered assembly and autonomous disassembly, respectively, within ~270 min (**Fig. 2e** and **S12-14**†). This tunability of the transiently stable controlled aggregated state via control over disassembly kinetics represents a significant advance towards achieving temporal functionality in dynamic self-assembled systems.

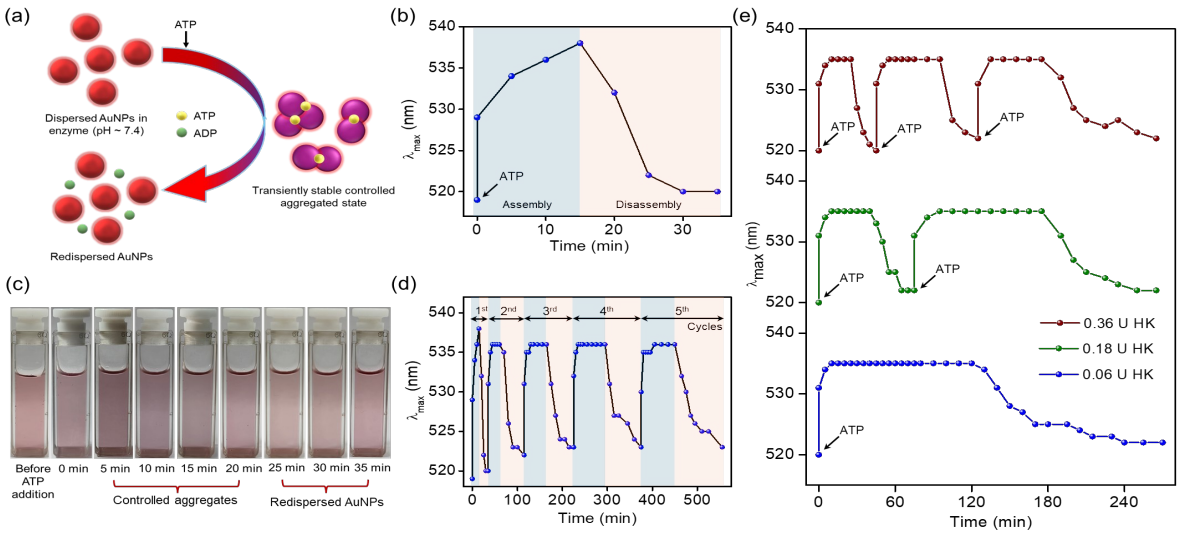

Figure 2. Self-assembly of AuNPs through pathway I (transient assembly). (a) Schematics showing the excess HK-driven autonomous reversibility in ATP-triggered dynamic self-assembly process. The reaction mixture contained 3 mL of 6 nM AuNPs, 5 μM of ATP, and 0.36 units of HK enzyme (excess). (b) A plot showing the temporal change in the λ_{max} of AuNPs during one cycle of the self-assembly process. (c) Time-dependent optical photographs showing the dynamic controlled aggregation of AuNPs in pathway I (transient assembly). (d) With 0.36 units of HK enzyme, five cycles of ATP-triggered dynamic self-assembly process were achieved. (e) A plot showing the increase in the number of dynamic self-assembly cycles, with an increase in the concentration of HK enzyme, within a time of ~270 min.

Pathway II (transient disassembly): Excess ATP-driven autonomous reversibility

Pathway II (transient disassembly) involves autonomous assembly driven by an excess of the assembling trigger (ATP), coupled with triggered disassembly by the disassembling trigger (HK enzyme). In this pathway, an excess of ATP was added in the initial stage to achieve its long-term dominance over the opposing disassembling HK trigger. And, to ensure the transient dominance of the disassembling HK trigger and thus enabling disassembly, the entire self-assembly process was performed at pH ~ 3.5, where the aggregation power of ATP is weak. Under these conditions, assembly occurs autonomously without the need for continuous addition of ATP, while disassembly is induced upon each addition of the HK trigger. This cycle of autonomous assembly and triggered disassembly continues until the ATP concentration falls below the threshold required for aggregation (**Scheme 2**). As the assembly cycle dominates in pathway II, the aggregation of AuNP proceeds to complete precipitation (plasmonically-off state) due to the excess ATP present. In a representative experiment, an excess ATP concentration (250 μM) was added to a 3 mL solution of ~6 nM AuNPs, causing instant aggregation between ATP and AuNP, as indicated by a visible color change from wine-red to purple and a red shift of ~18 nm in the plasmon band (**Fig. 3a,b** and **S15**†). Eventually, the ATP-AuNP aggregates fully precipitated from the solution within 8 h. DLS studies further confirmed rapid aggregation followed by precipitation, with hydrodynamic diameters increasing from ~10 to ~154 nm and eventually to ~1080 nm (**Fig. 3c**). Subsequent addition of 3 units of HK and ~250 equivalents of glucose (G) triggered enzymatic dephosphorylation of ATP to ADP, resulting in rapid redispersion of the ATP-AuNP precipitates. Based on zeta potential studies (**Fig. S16**†), we anticipated that the electrostatic accumulation of negatively charged HK at positively charged AuNP interfaces enhances its local concentration, generating a proximity-driven kinetic advantage that preferentially promoted dephosphorylation of surface-bound ATP over ATP in the bulk phase. However, redispersion was incomplete due to the excess ATP present in the system, which immediately triggered re-assembly followed by precipitation of the dispersed AuNPs (**Fig. 3b-d**). The dominance of excess ATP was further favored by the lower activity of HK at pH 3.5, as revealed by the pH-dependent stability studies (**Fig. S17**†). As reported before, a partial denaturing of HK was observed at pH 3.5.[50] But, HK still maintains limited catalytic activity at pH 3.5, allowing for occasional, low-affinity binding for ATP to ADP conversion. However, due to significant loss of activity over time at pH 3.5, HK behaves less as an efficient catalyst and more as a stoichiometric reagent. This explains why the addition of HK does not monotonically lead to the thermodynamic endpoint of a dispersed state, and a complete redispersion of AuNPs was observed only after the addition of a threshold amount of HK in the system (**Fig. S18**†). Further, no significant influence of glucose was observed on the disassembly step in Pathway II (**Fig. S19†**). In this way, the dominance of the assembling trigger was quickly restored after the transient action of the disassembling HK trigger. This autonomous assembly–triggered disassembly cycle was sustained until ATP amounts decreased below the threshold required for inducing aggregation (**Fig. 3d**). In the presence of 250 μM ATP, three cycles of reversible assembly and disassembly were achieved (**Fig. 3d** and **S20**†), with a shuttling between dispersed and completely precipitated states (**Fig. 3**).

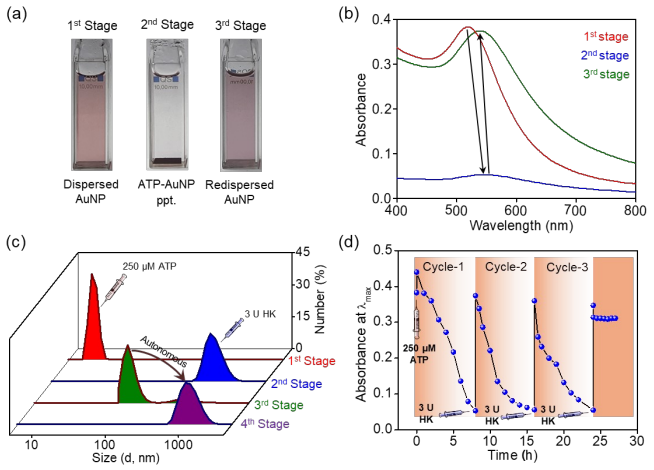

Figure 3. Autonomous self-assembly of AuNPs through pathway II (transient disassembly). (a) Optical photographs show the dispersed (1st stage), self-assembled (2nd stage), and redispersed (3rd stage) stages of autonomous self-assembly of AuNPs. The assembly step was triggered by ATP (250 μM), and the disassembly step was initiated by the HK enzyme (3 units). The corresponding changes in the (b) UV-vs absorption and (c) hydrodynamic diameter (DLS data) are shown. (d) Three cycles of autonomous self-assembly process were achieved with 250 μM ATP.

The dynamic interplay between the dominant assembly and transiently activated disassembly enables multiple reversible cycles of aggregation and redispersion. Now, the number of autonomous-assembly — triggered-disassembly cycles can be tuned by controlling the concentration of the aggregating trigger, ATP. For this, the self-assembly of AuNPs was performed in the presence of increasing concentrations of ATP (250 μM - 1 mM), while the disassembly in each cycle was triggered by the addition of 3 units of HK enzyme. (**Fig. 4** and **S20-24**†). The number of cycles increased from 3 to 8, as the ATP concentration was increased from 250 μM to 1 mM (**Fig. 4** and **S20-24**†). Interestingly, at 1 mM ATP concentration, a complete shuttling between plasmonically-off (aggerated) and plasmonically-on (dispersed) states was observed, along with negligible damping in the AuNP absorbance even after 8 cycles. Also, it was noticed that the assembly time increased and the extent of aggregation decreased toward the later cycles (**Fig. 4**). This can be attributed to the constant consumption of ATP across cycles, which reduces its effective concentration and slows the assembly kinetics over time. Notably, pH remained essentially constant throughout the multiple assembly-disassembly cycles, confirming that the dynamics of the system was controlled primarily by the availability and action of chemical triggers. Thus, these results highlight a novel dynamic self-assembly process wherein, despite the disassembly step proceeding faster, the autonomous assembly pathway dominates due to the initial excess of the assembling trigger. This system-level design enables tunable reversibility and temporal control, key features for realizing chemically programmed functions in artificial self-assembled systems.

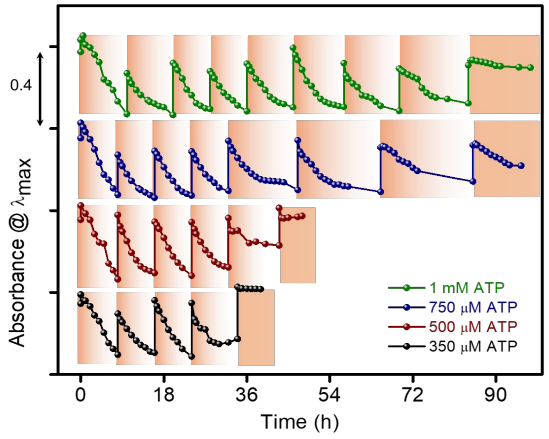

Figure 4. A plot showing the increase in the number of autonomous assembly — triggered disassembly cycles (via pathway II), with an increase in the concentration of ATP-trigger.

Comparative analysis of pathway I (transient assembly) and pathway II (transient disassembly)

Both pathway I (transient assembly) and pathway II (transient disassembly) resulted in the autonomous reversibility in ATP-AuNP self-assembly by exploiting the transient interplay between dominant and opposing triggers. The key difference lies in which process (assembly or disassembly) is autonomously driven by the excess trigger. Pathway I (transient assembly) features autonomous disassembly driven by an excess of HK, with a transient assembly triggered by ATP addition. Here, the enzymatic dephosphorylation of ATP to ADP maintains AuNPs in a controlled aggregate state (plasmonically-on state), and a transient action of ATP induces reversible aggregation. The transient dominance of ATP-triggered assembly was enabled by reaction conditions (pH ~ 7.4) that accelerate the aggregation power of ATP, allowing reversible cycling between dispersed and controlled aggregate states. On the contrary, in pathway II (transient disassembly), autonomous assembly was achieved through an excess of the aggregating trigger (ATP), while disassembly was triggered enzymatically via HK. The long-term dominance of ATP ensures rapid and complete aggregation of AuNPs, resulting in their precipitation (plasmonically off state). The transient dominance of HK-mediated disassembly was enabled by reaction conditions (pH ~ 3.5) that moderate the aggregation power of ATP, allowing reversible cycling between aggregated and dispersed states until ATP is depleted below the threshold required for aggregation (HPLC analysis reveals that a quantitative conversion of 250 μM ATP to ADP occurs after the third addition of HK, enabling the complete redispersal of AuNPs after three cycles. **Fig. S25**[†]). This comparative framework shows the versatility of self-assembly control, achieved by tuning the relative concentrations and activities of assembly and disassembly triggers under carefully optimized reaction conditions.

Conclusions

A biomimetic dynamic self-assembled system based on AuNP and ATP was developed that exhibits multiple autonomous, reversible assembly–disassembly cycles. Assembly occurs through electrostatic attraction between oppositely charged ATP and AuNPs, while disassembly is driven by HK-catalyzed dephosphorylation of ATP to ADP, which weakens this attraction. The system shows complete and reversible transitions between dispersed and precipitated AuNP states, a rare among nanoparticle-based dynamic assemblies. Autonomous reversibility was achieved via two pathways by pre-establishing the dominance of either the assembling or disassembling trigger. Appropriate pH conditions balanced the dominant and transient actions of the triggers, enabling autonomous reversibility in the self-assembly process. In pathway I (transient assembly), excess HK maintained autonomous disassembly, with transient assembly triggered by ATP addition. In pathway II (transient disassembly), excess ATP sustained autonomous assembly, with transient disassembly induced by HK addition. Notably, the nature of the self-assembled states was different in the two pathways: pathway I (transient assembly) produced switching between dispersed and plasmonically active, controlled aggregate states of AuNPs, whereas pathway II (transient disassembly) yielded reversible transitions between dispersed and fully precipitated states of AuNPs. Further, balancing the competing kinetics of the triggers allowed tuning of aggregate lifetimes from minutes to hours, a feature crucial for realizing temporal functions from dynamic self-assembled states. Our work demonstrates how careful regulation of trigger concentrations and kinetic balance can install autonomous reversibility in a self-assembly process. Overall, this study presents a versatile model for understanding pathway-dependent autonomous reversibility in synthetic and biomimetic self-assembled systems.

Author contributions

S. R. synthesized and characterized AuNPs. All the self-assembly studies were performed by S. R. and S.T. All authors contributed to the discussion, writing, and provided feedback on the manuscript. P. P. P. conceived the project and coordinated the research.

Conflicts of interest

There are no conflicts to declare.

Data availability

The data supporting this article have been included as part of the ESI.

Acknowledgements

The authors acknowledge the financial support from ANRF (Erstwhile SERB) India Grant CRG/2023/00171. S. R. and S. T thank DST INSPIRE and UGC respectively for Ph.D. fellowships. The authors also acknowledge Biswajit Behera and Prof. Jayant Udgaonkar for assisting us with CD measurements, and Shreya Mahato and Prof. Amrita Hazra for assisting us with HPLC measurements.

References

1 G. M. Whitesides and B. Grzybowski, *Science* 2002, **295**, 2418–2421.
2 J. -M. Lehn, *Science* 2002, **295**, 2400– 2403.
3 B. A. Grzybowski, K. Fitzner, J. Paczesny and S. Granick, *Chem. Soc. Rev.* 2017, **46**, 5647−5678.
4 D. Philp and J. F. Stoddart, *Angew. Chem., Int. Ed.* 1996, **35**, 1154−1196.
5 R. F. Ismagilov, A. Schwartz, N. Bowden and G. M. Whitesides, *Angew. Chem. Int. Ed.* 2002, **41**, 652–654.
6 C. H. Chen, E. L. Hsu and S. I. Stupp, *Bone* 2020, **141**, 115565.
7 S. Mann, *Acc. Chem. Res.* 2012, **45**, 2131−2141.
8 T. Aida, E. W. Meijer and S. I. Stupp, *Science* 2012, **335**, 813–817.
9 A. Sorrenti, J. Leira-Iglesias, A. J. Markvoort, T. F. A. de Greef and T. M. Hermans, *Chem. Soc. Rev.* 2017, **46**, 5476−5490.
10 S. Dhiman and S. J. George, *Bull. Chem. Soc. Jpn.* 2018, **91**, 687–699.
11 A. Rao, S. Roy, V. Jain and P. P. Pillai, *ACS Appl. Mater. Interfaces* 2023, **15**, 25248–25274.
12 G. Ashkenasy, T. M. Hermans, S. Otto and A. F. Taylor, *Chem. Soc. Rev.* 2017, **46**, 2543−2554.
13 B. A. Grzybowski and W. T. S. Huck, *Nat. Nanotechnol.* 2016, **11**, 585−592.
14 R. Merindol and A. Walther, *Chem. Soc. Rev.* 2017, **46**, 5588–5619.
15 K. Gentile, A. Somasundar, A. Bhide and A. Sen, *Chem* 2020, **6**, 2174–2185.
16 K. Das, L. Gabrielli and L. J. Prins, *Angew. Chem. Int. Ed.* 2021, **60**, 20120–20143.
17 M. W. Mosesson and M. Kaminski, *Blood Coagul. Fibrinolysis* 1990, **1**, 475-478.
18 K. E. Kadler, D. F. Holmes, J. A. Trotter and J. A. Chapman, *Biochem J* 1996, **316**, 1–11.
19 T. Mitchison and M. Kirschner, *Nature* 1984, **312**, 237–242.
20 M. F. Carlier, D. Pantaloni and E.D. Korn, *J. Biol. Chem.* 1984, **259**, 9983–9986.
21 J. Leira-Iglesias, A. Tassoni, T. Adachi, M. Stich and T. M. Hermans, *Nat. Nanotechnol.* 2018, **13**, 1021–1027.
22 S. N. Semenov, L. J. Kraft, A. Ainla, M. Zhao, M. Baghbanzadeh, V. E. Campbell, K. Kang, J. M. Fox and G. M. Whitesides, *Nature* 2016, **537**, 656–660.
23 M. G. Howlett, A. H. J. Engwerda, R. J. H. Scanes and S. P. Fletcher, *Nat. Chem.* 2022, **14**, 805–810.
24 A. Reja, S. Jha, A. Sreejan, S. Pal, S. Bal, C. Gadgil and D. Das, *Nat. Commun.* 2024, **15**, 9980.
25 T. Sangchai, S. Al. Shehimy, E. Penocchio and G. Ragazzon, *Angew. Chem. Int. Ed.* 2023, **62**, e202309501.
26 C. Pezzato and L. J. Prins, *Nat. Commun.*, 2015, **6**, 7790.
27 T. Heuser, A.-K. Steppert, C. M. Lopez, B. Zhu and A. Walther, *Nano Lett.* 2015, **15**, 2213−2219.
28 J. H. van Esch, R. Klajn and S. Otto, *Chem. Soc. Rev.* 2017, **46**, 5474–5475.
29 N. Giuseppone and A. Walther, *Out-of-equilibrium (supra) molecular systems and materials*; Wiley-VCH GmbH: Weinheim, Germany, 2021.
30 S. Maiti, I. Fortunati, C. Ferrante, P. Scrimin and L. J. Prins, *Nat. Chem.* 2016, **8**, 725−731.
31 J. Boekhoven, W. E. Hendriksen, G. J. M. Koper, R. Eelkema and J. H. van Esch, *Science* 2015, **349**, 1075−1079.
32 J. Rodon-Fores, M. A. Würbser, M. Kretschmer, B. Rieß, A. M. Bergmann, O. Lieleg and J. Boekhoven, *Chem. Sci.* 2022, **13**, 11411–11421.
33 A. Sorrenti, J. Leira-Iglesias, A. Sato and T. M. Hermans, *Nat. Commun.* 2017, **8**, 15899.
34 Y. Cao, L. Gabrielli, D. Frezzato and L. J. Prins, *Angew. Chem. Int. Ed.* 2023, **62**, e202215421.
35 A. Rao, S. Roy and P. P. Pillai, *Langmuir* 2021, **37**, 1843−1849.
36 S. Roy, R. K. Kashyap and P. P. Pillai, *J. Phys. Chem. C* 2023, **127**, 10355–10365.
37 K. K. Nakashima, J. F. Baaij and E. Spruijt, *Soft Matter* 2018, **14**, 361–367.
38 S. Roy, L. Gravener, D. Philp and E. R. Kay, *Angew. Chem. Int. Ed.* 2023, **62**, e202217613
39 S. Cao, L. Caire da Silva and K. Landfester, *Angew. Chem. Int. Ed.* 2022, **61**, e202205266.
40 L. Saile, K. Dai, M. D. Pol, T. Pramod, R. Thomann and C. G. Pappas, *Angew. Chem. Int. Ed.* 2025, **64**, e202508481.
41 R. K. Grötsch, A. Angı, Y. G. Mideksa, C. Wanzke, M. Tena-Solsona, M. J. Feige, B. Rieger and J. Boekhoven, *Angew. Chem. Int. Ed.* 2018, **57**, 14608.
42 B. G. P. van Ravensteijn, W. E. Hendriksen, R. Eelkema, J. H. van Esch and W. K. Kegel, *J. Am. Chem. Soc.* 2017, **139**, 9763–9766.
43 R. K. Grötsch, C. Wanzke, M. Speckbacher, A. Angı, B. Rieger and J. Boekhoven, *J. Am. Chem. Soc.* 2019, **141**, 9872–9878.
44 B. G. P. van Ravensteijn, I. K. Voets, W. K. Kegel and R. Eelkema, *Langmuir* 2020, **36**, 10639–10656.
45 S. Dhiman, A. Jain and S. J. George, *Angew. Chem. Int. Ed.* 2017, **56**, 1329–1333.
46 T. Bian, A. Gardin, J. Gemen, L. Houben, C. Perego, B. Lee, N. Elad, Z. Chu, G. M. Pavan and R. Klajn, *Nat. Chem.* 2021, **13**, 940– 949.
47 J. Israelachvili, *Intermolecular and Surface Forces*; Academic Press: New York, 1991.
48 S. Roy and P. P. Pillai, *Langmuir* 2023, **39**, 12967-12974.
49 S. Roy, V. S. S. Adury, A. Rao, S. Roy, A. Mukherjee and P. P. Pillai, *Angew. Chem., Int. Ed.* 2022, **61**, e202203924.
50 P. Kumar, A. Tiwari and R. Bhat, *J Biol Chem*. 2004, **279**, 32093–32099.

View Article Online
DOI: 10.1039/D6SC01862A

View Article Online
DOI: 10.1039/D6SC01862A

Data availability statement

The data supporting this article have been included as part of the ESI.